


Preparation of carbon quantum dots biofilm and adsorption of heavy metal Cu²⁺

American Journal of Chemistry
Vol. 10, No. 1, 12-21, 2025
e-ISSN:2616-5244



 **Jianting WEI**

School of Food Science and Technology, Shihezi University, Shihezi, Xinjiang, 832003, China.
Email: 1793118415@qq.com

ABSTRACT

Currently, seawater is seriously polluted by Cu²⁺, thus the development of safe and efficient Cu²⁺ removal materials is important for maintaining the safety of marine ecology. In this study, we utilized reed and urea as raw materials, synthesizing carbon quantum dots (CQDs) and nitrogen-doped carbon quantum dots (N-CQDs) through the hydrothermal method. Then, we analyzed their performance in Cu²⁺ detection and absorbance. Both the CQDs and N-CQDs exhibited excellent fluorescent properties, with maximum excitation wavelengths at 325 nm and corresponding emission wavelengths at 400 nm. Nitrogen doping enhanced the fluorescence intensity and stability of CQDs. Various metal ions were tested for their fluorescence-quenching effects on CQDs and N-CQDs. The results indicated that the N-CQDs exhibited strong adsorption capacity towards Cu²⁺, showing a good linear relationship at Cu²⁺ concentrations ranging from 0 to 50 μmol/L with a detection limit of 1.081 μmol/L. Additionally, we prepared a CQDs-biofilm using 3% chitosan as raw material and evaluated the adsorption of Cu²⁺ by the N-CQDs biofilm. The findings revealed that the Cu²⁺ adsorption rate of the N-CQD biofilm ranged from 28% to 67%. This CQD-biofilm is significant for trace detection and pollution control of Cu²⁺ in aqueous media.

Keywords: Carbon quantum dot biofilm, Carbon quantum dots, Copper contamination, Fluorescence quenching, Nitrogen doping.

DOI: 10.55284/ajc.v10i1.1359

Citation | WEI, J. (2025). Preparation of carbon quantum dots biofilm and adsorption of heavy metal Cu²⁺. *American Journal of Chemistry*, 10(1), 12–21.

Copyright: © 2025 by the author. This article is an open access article distributed under the terms and conditions of the Creative Commons Attribution (CC BY) license (<https://creativecommons.org/licenses/by/4.0/>).

Funding: This study received no specific financial support.

Institutional Review Board Statement: Not applicable.

Transparency: The author confirms that the manuscript is an honest, accurate, and transparent account of the study; that no vital features of the study have been omitted; and that any discrepancies from the study as planned have been explained. This study followed all ethical practices during writing.

Competing Interests: The author declares that there are no conflicts of interests regarding the publication of this paper.

History: Received: 16 December 2024/ Revised: 29 January 2025/ Accepted: 17 February 2025/ Published: 14 March 2025

Publisher: Online Science Publishing

Highlights of this paper

- We utilized reed and urea as raw materials, synthesizing carbon quantum dots (CQDs) and nitrogen-doped carbon quantum dots (N-CQDs) through the hydrothermal method.
- N2-CQDs exhibited excellent fluorescence properties for Cu²⁺ detection.
- N2-CQDs functionalised biofilm is significant for Cu²⁺ removal under seawater conditions.

1. INTRODUCTION

Heavy metals are a class of environmental contaminants that are widely distributed, readily bioconcentrated, highly toxic, and poorly biodegradable (Malik, Bashir, Qureashi, & Pandith, 2019). With the rapid development of industry, a large amount of heavy metal pollutants has entered the marine environment through surface runoff and coastal wastewater. Simultaneously, as human activities have increased, the effect of anthropogenic pollution on the accumulation of heavy metals in seawater has become more pronounced (Lim, Liu, Kim, & Son, 2018; Pooja, Singh, Thakur, & Kumar, 2019). More importantly, heavy metals such as Pb, Cd, As, and Hg. Seawater also poses a serious threat to terrestrial organisms and human health through the accumulation of biological enrichment and amplification in the food chain (Devi, Rajput, Thakur, Kim, & Kumar, 2019; Junaid, Batool, Harun, Akhter, & Shabbir, 2022). Therefore, it is important to remediate and remove heavy metals from seawater.

CQDs are a new class of carbon nanoparticles consisting mainly of carbon spheres with sizes below 10 nm (Athika et al., 2019). Compared with traditional semiconductor quantum dots, CQDs have many unique advantages, such as good biocompatibility, low toxicity, stable chemical properties and good water solubility. Therefore, CQDs have been widely used in various fields, including bioimaging, fluorescent probes, drug delivery, optoelectronic devices, water purification technology and heavy metal ion detection (Ye et al., 2017).

Chitosan (CS) is an alkaline natural polysaccharide and has been widely used in recent years, due to its advantages such as non-toxic, degradable, widely available, and film-forming properties (Athika et al., 2019; Cui, Ren, Sun, Liu, & Xia, 2021; Ye et al., 2017). In this study, we used inexpensive reed leaves as a carbon source to prepare CQDs and CQDs-functionalized biofilm, which is important for the remediation of Cu²⁺ in seawater and pollution prevention.

2. MATERIALS AND METHODS

2.1. Materials

Reeds were collected near the Fork River (Dezhou, China). Analytical-grade chemical reagents were purchased from Tianjin Kemiou Chemical Reagent Co. Ltd (Tianjin, China). Standard solutions of heavy metal were obtained from the National Reference Material Center (USA). Artificial seawater was purchased from Tangshan Municipal Yard (Tangshan, China).

2.2. Characterisation of CQDs and N-CQDs

2.2.1. Preparation of CQDs and N-CQDs

Reed leaves were thoroughly rinsed three times with deionized water to remove dust particles, dried, and pulverized. 2.5 g of powder was mixed with 60 ml of deionized water and boiled for 2 hours to obtain the reed solution. Afterwards, 10 ml of the reed solution was heated at 200 °C for 12 hours. At the end of the reaction, the solution was centrifuged at 12,000 rpm for 10 minutes and filtered with a 0.22 µm filter membrane to purify the product. The filtered solution was therefore the stock solution of CQDs, which was stored at 4 °C (Cai et al., 2018). As indicated in Table 1, the N-CQDs were prepared similarly to CQD fabrication technique but with the addition of urea.

Table 1. Naming of CQDs with different urea content.

Treatments	1	2	3	4
Urea addition (g)	0	0.1	0.5	1.0
CQD designations	CQDs	N ₁ -CQDs	N ₂ -CQDs	N ₃ -CQDs

2.2.2. Analysis of the Properties of CQDs and N-CQDs

The particle size distribution and the zeta potential were determined using dynamic light scattering (DLS). The Ultraviolet–visible spectroscopy (UV-Vis) spectra of CQDs and N-CQDs were analyzed in the range of 300–600 nm. The detection of the fluorescence (FL) properties was carried out using the following method: the slit widths of the incident wavelength and the emission wavelength were 2.5 nm and 5.0 nm, respectively, and the photomultiplier voltage was 400 V. The emission spectra were measured at different excitation wavelengths to determine the optimal excitation wavelength (Dragan & Geddes, 2012; Mindivan & Göktaş, 2023). The fluorescence quantum yield was determined using quinine sulfate as a reference (Lin, Deng, & Li, 2022).

2.3. Detection of Heavy Metal Ions by CQDs and N-CQDs

At room temperature, the stock solutions of CQDs and N-CQDs were diluted 100-fold with deionized water, and the fluorescence emission spectra were acquired at the optimal excitation wavelength, and the fluorescence intensity was recorded, which corresponds to the initial fluorescence intensity value of CQDs and N-CQDs and was set to F₀. The different metal ion solutions (Co²⁺, Pb²⁺, Ni²⁺, Cd²⁺, Cu²⁺, Ba²⁺, Ag²⁺, Fe³⁺, Hg²⁺ and As⁵⁺) were prepared at a concentration of 400 mg/L. Then, the 50-fold diluted CQDs and N-CQDs were mixed with different metal cation solutions in equal proportions, and the change in fluorescence intensity was recorded as F. The degree of fluorescence quenching was calculated using a value of F₀-F/F₀ (Das et al., 2017).

In the quantitative detection of Cu²⁺ ions, different concentrations of Cu²⁺ solutions (0~1000 μmol/L, equivalent to 0~17 mg/L) were mixed with the N-CQDs solution in equal proportions, and vortexed and mixed for 10 s at room temperature. The fluorescence intensities of the mixed system at the optimal excitation wavelength were detected to analyse the detection range of Cu²⁺ and the linear relationship (Xiang-Yi et al., 2020).

2.4. N-CQDs Biofilm Preparation

After dissolving CS at a volume fraction of 10% in acetic acid solution, 100-fold diluted N-CQDs solution was added, and the mixture was stirred for 80 minutes at 60 °C until it was completely dissolved. Next, 1% glycerol was added, and the mixture was magnetically stirred for an hour at room temperature until it was thoroughly mixed. Finally, it was centrifuged for 20 minutes at 6,000 rpm to eliminate any bubbles and create the CS film formation solution. Following the aforesaid procedure, the film-forming solutions with 1% CS, 2% CS, 3% CS, and 4% CS were made and designated as N-CQDs-1 to N-CQDs-4. The film-forming solution was distributed in a 90 mm diameter Petri dish and dried at 45 °C for 12 hours to form a film (Tian, Qin, & Xie, 2023).

2.5. Analysis of the Adsorption of N-CQDs Biofilm

A series of Cu²⁺ solutions with concentration gradients (1-5 mg/L) were configured, N-CQDs biofilms of the same size were placed in them, and the residual Cu²⁺ content on the solutions after adsorption for different periods (5 min, 10 min, 15 min and 20 min) was determined using inductively coupled plasma emission ICP spectrometry (Han et al., 2021).

3. RESULTS AND DISCUSSION

3.1. Preparation and Characterization of CQDs and N-CQDs

3.1.1. Preparation and DLS Particle Size Distribution and Zeta Potential of CQDs and N-CQDs

As shown in Figure 1, the synthetic CQDs and N-CQDs solutions showed yellow color under visible light, and the solutions of N-doped CQDs were reddish-brown color. Both CQDs and N-CQDs emitted bluish fluorescence under UV light, further indicating the successful synthesis of CQDs.

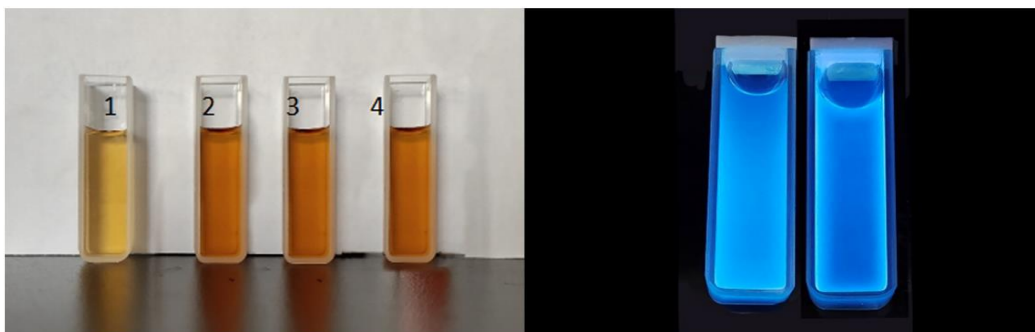


Figure 1. The digital photos of CQDs and N-CQDs under visible and ultraviolet light.

The particle size distributions of CQDs and N₂-CQDs are shown in Figure 2(a). The diameter range of CQDs is 4.8–11.6 nm with an average size of about 7.8 nm and that of N₂-CQDs is 5.6–13.5 nm, with an average size of about 8.4 nm. The zeta potential of CQDs was measured to be -14.5 mV, and that of N₂-CQDs was -23.7 mV, exhibiting high dispersion stability.

As shown in Figure 2(b), both CQDs and N₂-CQDs showed absorption in a broader range from 220 to 580 nm, with CQDs showing absorption peaks at 280 nm and 330 nm and N₂-CQDs showing obvious absorption peaks at 285 nm and weak absorption peaks at 315 and 335 nm. The UV absorption of CQDs and N₂-CQDs can be attributed to the $n-\pi^*$ and $\pi-\pi^*$ jumps of the carbonyl (C=O/C=C) and amino groups in them (Ganguly, Das, Banerjee, & Das, 2019). The increase in $\pi-\pi^*$ jumps in the N-doped CQDs increases the absorption in the UV and visible regions (Rong, Zhang, Wang, & Chen, 2017). The fluorescence quantum yields of the reed-CQDs and N₂-CQDs were also calculated, and the results showed that the fluorescence quantum yield of the prepared CQDs was 5.21% and that of the N₂-CQDs was 7.35%, respectively.

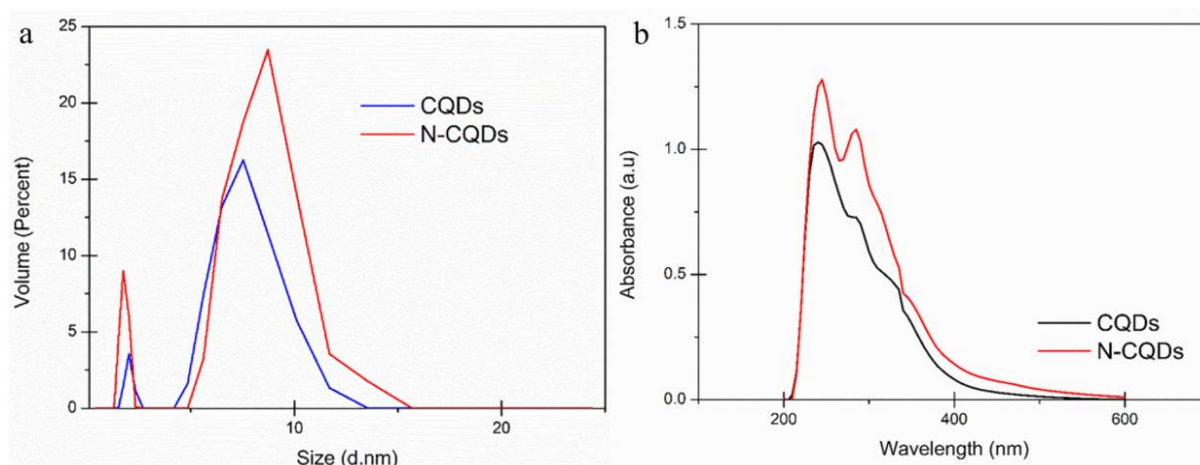


Figure 2. Particle size distribution and UV-Vis absorption spectra.

Note: (a). Particle size distribution. (b) UV-Vis absorption spectra.

3.1.2. FL Emission Spectra of CQDs and N-CQDs

Both CQDs and N₂-CQDs display a similar fluorescence behavior, where fluorescence intensity increases gradually as the excitation wavelength ranges from 285 nm to 325 nm. Conversely, as the excitation wavelength is further increased from 325 nm to 385 nm, the maximum emission peaks shift towards longer wavelengths and the fluorescence intensity decreases gradually. This behavior is attributed to variations in the sizes of the CQDs and the presence of different surface emission sites, which stem from the prevalence of polar functional groups (-OH, -COOH, and -NH₂) on the CQDs' surface. These functional groups facilitate electron transitions that result in relaxation phenomena in polar solvents such as deionized water, leading to variations in the fluorescence emission observed at different excitation wavelengths (J. Li et al., 2013). The excitation wavelength-dependent emission characteristics observed in both carbon quantum dots are a distinctive trait of carbonaceous materials, arising from the diverse emission sites present in their surface structures (Omer, Tofiq, & Ghafoor, 2019).

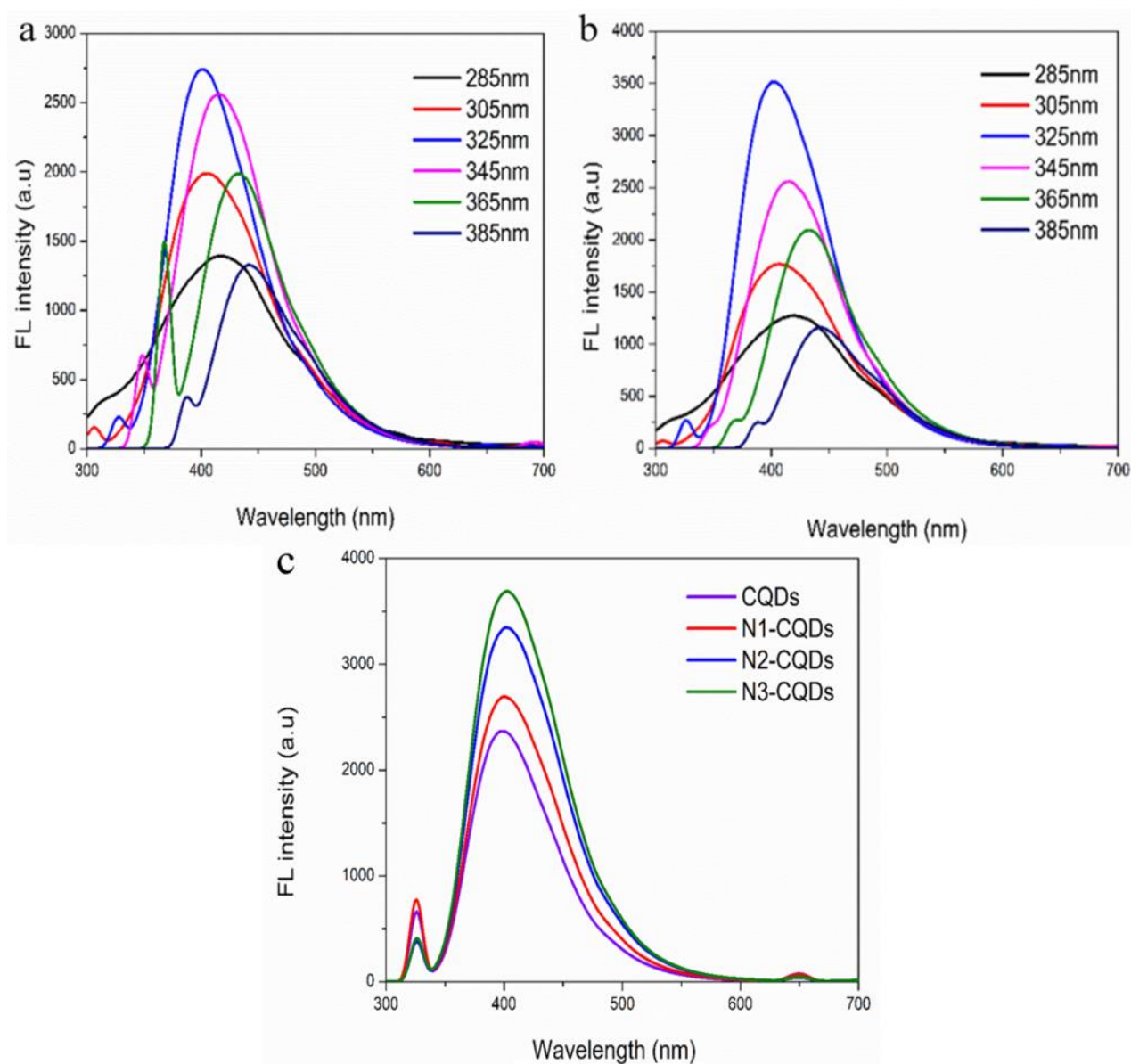


Figure 3. Fluorescence emission spectra of CQDs.

Note: (a) and (b) Fluorescence emission spectra of CQD and N₂-CQDs at different excitation wavelengths, respectively. (c) Fluorescence emission spectra at 325 nm.

The fluorescence emission spectra of CQDs and N-CQDs were examined at an excitation wavelength of 325 nm, because this is the optimal excitation wavelength as depicted in Figure 3(a) and 3(b). A comparison of the fluorescence properties revealed that the N-CQDs exhibited a notably higher fluorescence intensity at the optimal excitation wavelength compared to the CQDs as illustrated in Figure 3(c). This enhancement in fluorescence intensity can be attributed to the increased presence of aerobic functional groups (-OH, -COOH, and -NH₂) on the surface of N-CQDs resulting from nitrogen doping, as reported in previous studies (Mao, Xue, & Han, 2021)

3.2. Fluorescence Stability of CQDs and N-CQDs

The CQDs showed excellent stability, and the fluorescence intensity basically remained stable in 2-24h, which laid the foundation for its application as illustrated in Figure 4(a). Furthermore, the impact of varying pH levels on the fluorescence intensity of CQDs and N₂-CQDs was explored. Results depicted in Figure 4b demonstrated that within the pH range of 5 to 8, both CQDs and N₂-CQDs exhibited minimal fluctuations in fluorescence intensity, indicating stability. Conversely, at pH levels below 3 or above 9, the fluorescence intensity of both types of quantum dots fluctuated more significantly. In acidic conditions, the competition for adsorption sites between hydrogen ions and metal ions, coupled with a high concentration of H⁺ ions disrupting ionic equilibrium, led to increased surface defects and subsequent reduction in fluorescence intensity (Lei et al., 2019). On the other hand, alkaline solutions induced a decrease in fluorescence intensity due to the presence of excess -OH ions altering the number of surface C=O groups such as carboxyl groups. Notably, extreme pH conditions exerted a more pronounced influence on the fluorescence intensity of carbon quantum dot solutions. Additionally, N₂-CQDs exhibited greater stability in response to pH changes compared to CQDs, as evidenced by the minimal impact on their overall fluorescence intensity.

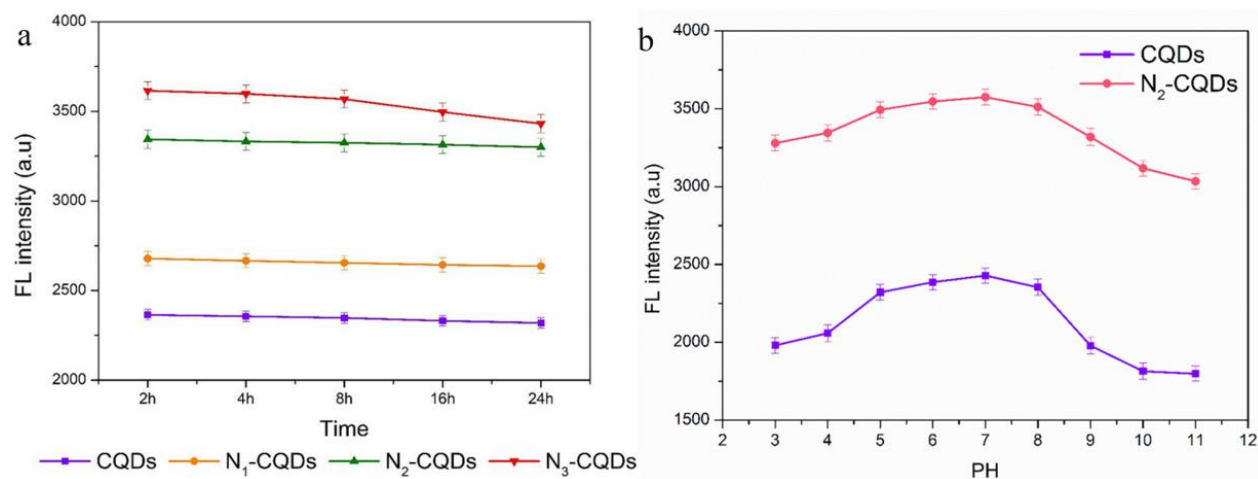


Figure 4. Effect of time and pH on the fluorescence intensity of CQDs and N₂-CQDs.

3.3. Detection of Metal Ions by CQDs and N₂-CQDs

To investigate the ability of CQDs and N₂-CQDs to detect different metal ions, ten different metal ions were used for selectivity assay. The results revealed a substantial disparity between the interactions of CQDs and N₂-CQDs with Fe³⁺ and Cu²⁺ compared to blank (Figure 5a). N₂-CQDs showed the greatest fluorescence quenching effect in the heavy metal detection and were therefore selected for subsequent studies (Figure 5b). Notably, Fe³⁺ and Cu²⁺ exhibited a pronounced quenching effect on the fluorescence of both CQDs and N₂-CQDs, surpassing the impact of other metal ions tested. This quenching phenomenon can be attributed to the strong surface interactions

of metal ions with functional groups on the CQDs, such as hydroxyl, amino, and carbonyl groups, impeding the radiative electron transitions within the carbon quantum dots and thereby suppressing their fluorescence emission. Moreover, the introduction of Cu^{2+} resulted in a more marked distinction between N2-CQDs compared to CQDs, indicating an enhanced adsorption capacity of N2-CQDs towards Cu^{2+} . This enhanced affinity can be linked to structural modifications induced by the addition of urea, leading to an increase in functional groups like amino, hydroxyl, and carbonyl on the N2-CQDs, thereby intensifying the interactions with Cu^{2+} and boosting the fluorescence quenching effect of Cu^{2+} on N2-CQDs. Under the optimized analytical conditions, based on the fluorescence quenching effect of Cu^{2+} on N2-CQDs, Cu^{2+} can be quantitatively detected by the prepared CQDs. Analyzing the fluorescence quenching effect of different concentrations of Cu^{2+} on N2-CQDs, the change of fluorescence intensity is shown in Figure 5c, and the fluorescence value decreases gradually with the increase of Cu^{2+} concentration, and the larger the ion concentration is, the more the fluorescence intensity decreases, and the stronger the bursting effect is. Due to the existence of the passivation groups -OH and -NH₂ on the surface of carbon quantum dots interacting with Cu^{2+} in a coordinated manner, leading to the bursting of the fluorescence of carbon quantum dots, as the concentration of Cu^{2+} increases, the more -OH and -NH₂ interact with it, further changing the surface defects of the carbon quantum dots, and thus the better the bursting effect (J. Y. Li, Han, & Yang, 2021).

The relationship between the relative fluorescence intensity F_0/F of N2-CQDs and the concentration of Cu^{2+} was investigated in Figure 5d, and the results showed that there was a good linear relationship between Cu^{2+} in the range of 10-50 $\mu\text{mol/L}$ and the relative fluorescence intensity F_0/F of the N2-CQDs, with the standard curve equation of $y = -0.0042x + 0.859$, $R^2 = 0.9977$, and the detection limit was The above results showed that N2-CQDs can be used as a fluorescent probe for the detection of Cu^{2+} .

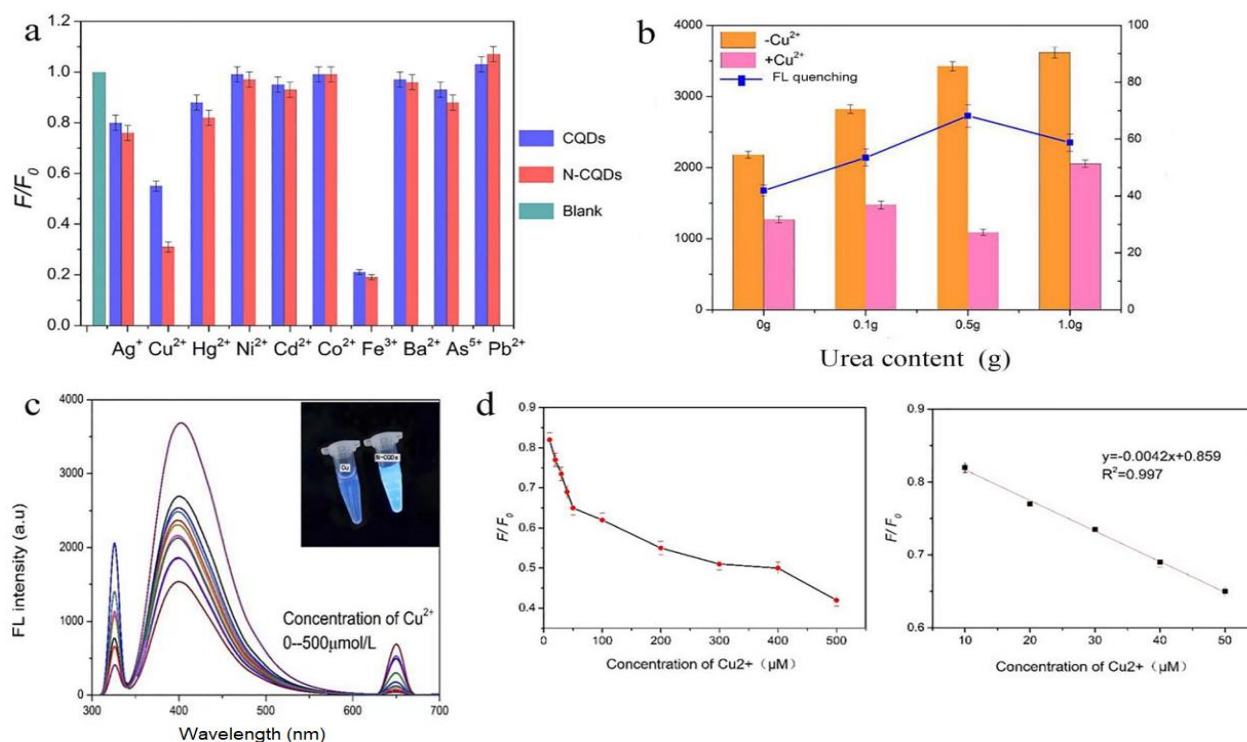


Figure 5. Performance of CQDs and N2-CQDs detecting heavy metals.

- Note:** (a) Quenching effect of different metal ions (100 mg/L) on the fluorescence of CQDs and N2-CQDs. (b) Effect of different urea additions on the effect of CQDs on the action of Cu^{2+} . (c) Fluorescence quenching of N2-CQDs by different concentrations of Cu^{2+} (inset shows fluorescence comparison of N2-CQDs before and after Cu^{2+} addition under UV light). (d) Relationship curve between FL emission intensity as a function of different concentration of Cu^{2+} .

3.4. Preparation of N₂-CQDs Functionalized Chitosan Biofilms

The biofilms with the best film-forming effect were selected according to their thickness, hardness and viscosity. The results showed that the biofilm containing 3% chitosan was moderate thickness, smooth and easy to tear, so the N₂-CQDs biofilm prepared with 3% chitosan was selected for the subsequent experiments. As shown in Figure 6(a), the N₂-CQDs coated membrane emitted a yellowish-brown color under visible light irradiation. Under UV irradiation, it emitted a blue color in the absence of Cu²⁺ ions (Figure 6b). When the Cu²⁺ ions were dropped into the N₂-CQDs biofilm, the spectrum tended to become darker, i.e. fluorescence quenching (Figure 6c).

Then, the adsorption of Cu²⁺ by N₂-CQDs biofilm was investigated, and the results showed that the adsorption and removal effect of biofilm on Cu²⁺ in artificial seawater was related to the adsorption time and concentration of Cu²⁺. With the increase of the adsorption time of Cu²⁺ by biofilm, the Cu²⁺ content in artificial seawater showed a decreasing trend. The Cu²⁺ content of the artificial seawater with an initial content of 1 mg/L Cu²⁺ was 0.565 mg/L after 20 min of adsorption with an adsorption rate of 43.5%. For the seawater with an initial content of 2 mg/L Cu²⁺, the Cu²⁺ content was 0.656 mg/L after 20 min of adsorption, with an adsorption rate of 67.2%. In the case of seawater containing 5 mg/L Cu²⁺, the Cu²⁺ content decreased to 3.604 mg/L after 20 min of adsorption, with an adsorption rate of 28%. Due to the small and thin area of the N₂-CQDs biofilm (Figure 6), the total amount of N₂-CQDs was limited, and the adsorption capacity reached near saturation, and with the release of N₂-CQDs, the adsorption capacity decreased after 5 min.

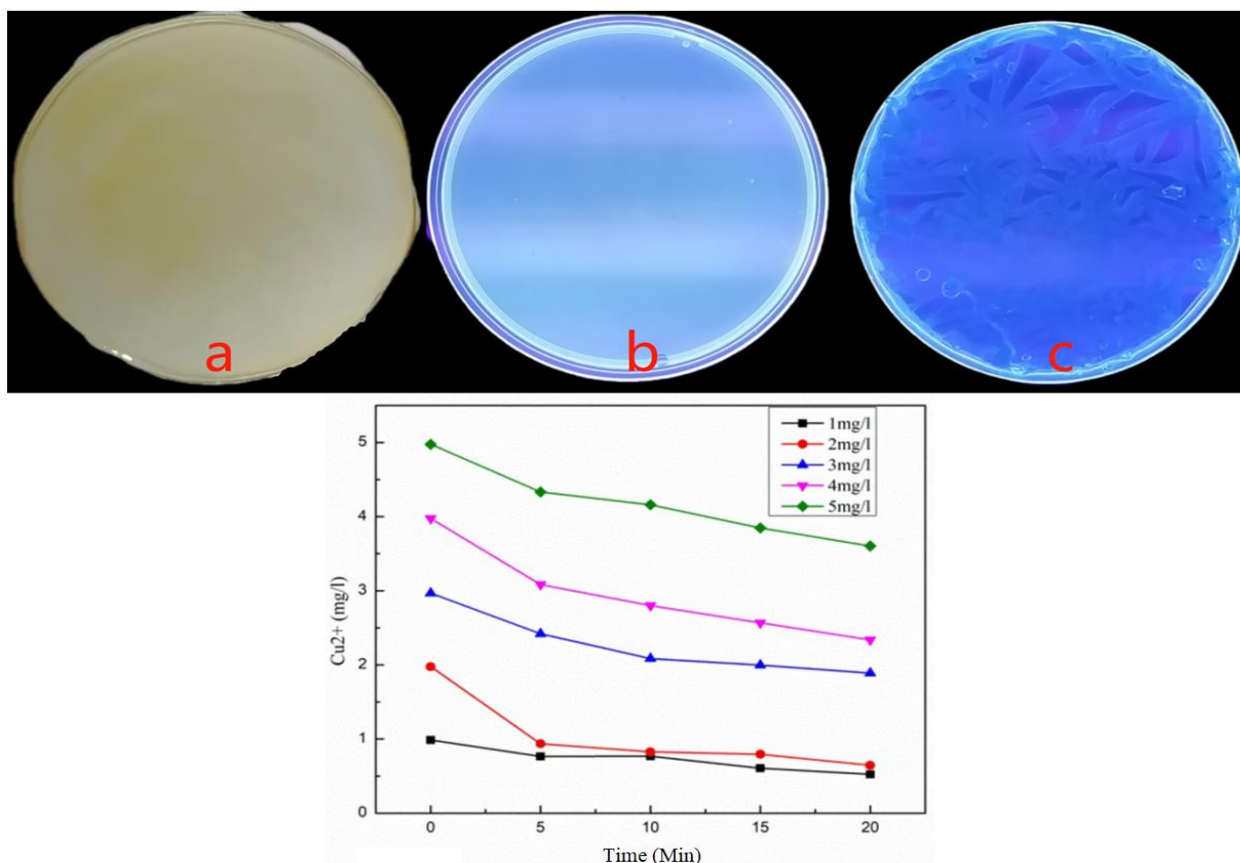


Figure 6. Fluorescence effect of copper adsorption by N₂-CQDs biofilm.

4. CONCLUSION

In conclusion, the N-CQDs were synthesized by hydrothermal method using cheap and renewable biomass reed leaves as a carbon source. The prepared N-CQDs had excitation wavelength-dependent emission properties and

emitted strong blue fluorescence under UV lamp irradiation, with an optimal excitation wavelength of 325 nm. Nitrogen doping improved the fluorescence intensity and storage stability of CQDs, and the N₂-CQDs had high adsorption capacity of Cu²⁺. The N₂-CQDs biofilm was prepared using 3% chitosan, while its Cu²⁺ adsorption rate was 28%~67%. This study developed a fluorescence analysis method for heavy metal ion content in adsorbed seawater to realize the rapid detection of Cu²⁺ ions in seawater, which is of great significance for trace detection and pollution prevention of Cu²⁺ in aqueous media.

REFERENCES

- Athika, M., Prasath, A., Duraisamy, E., Devi, V. S., Sharma, A. S., & Elumalai, P. (2019). Carbon-quantum dots derived from denatured milk for efficient chromium-ion sensing and supercapacitor applications. *Materials Letters*, 241, 156-159. <https://doi.org/10.1016/j.matlet.2019.01.064>
- Cai, Y., You, J., You, Z., Dong, F., Du, S., & Zhang, L. (2018). Profuse color-evolution-based fluorescent test paper sensor for rapid and visual monitoring of endogenous Cu²⁺ in human urine. *Biosensors and Bioelectronics*, 99, 332-337. <https://doi.org/10.1016/j.bios.2017.07.072>
- Cui, L., Ren, X., Sun, M., Liu, H., & Xia, L. (2021). Carbon dots: Synthesis, properties and applications. *Nanomaterials*, 11(12), 3419. <https://doi.org/10.3390/nano11123419>
- Das, P., Ganguly, S., Bose, M., Mondal, S., Das, A. K., Banerjee, S., & Das, N. C. (2017). A simplistic approach to green future with eco-friendly luminescent carbon dots and their application to fluorescent nano-sensor 'turn-off' probe for selective sensing of copper ions. *Materials Science and Engineering: C*, 75, 1456-1464. <https://doi.org/10.1016/j.msec.2017.03.045>
- Devi, P., Rajput, P., Thakur, A., Kim, K.-H., & Kumar, P. (2019). Recent advances in carbon quantum dot-based sensing of heavy metals in water. *TrAC Trends in Analytical Chemistry*, 114, 171-195. <https://doi.org/10.1016/j.trac.2019.03.003>
- Dragan, A. I., & Geddes, C. D. (2012). Metal-enhanced fluorescence: The role of quantum yield, Q, in enhanced fluorescence. *Applied Physics Letters*, 100(9). <https://doi.org/10.1063/1.3692105>
- Ganguly, S., Das, P., Banerjee, S., & Das, N. C. (2019). Advancement in science and technology of carbon dot-polymer hybrid composites: A review. *Functional Composites and Structures*, 1(2), 022001. <https://doi.org/10.1088/2631-6331/ab0c80>
- Han, M., Han, Y., Sun, M., He, L., He, J., & Bi, S. (2021). Adsorption of heavy metal ions by magnetic chitosan materials. *Liaoning Chemical Industry*, 50(1), 36-37.
- Junaid, H. M., Batool, M., Harun, F. W., Akhter, M. S., & Shabbir, N. (2022). Naked eye chemosensing of anions by Schiff bases. *Critical Reviews in Analytical Chemistry*, 52(3), 463-480. <https://doi.org/10.1080/10408347.2020.1806703>
- Lei, Y., Cui, Y., Huang, Q., Dou, J., Gan, D., Deng, F., . . . Wei, Y. (2019). Facile preparation of sulfonic groups functionalized Mxenes for efficient removal of methylene blue. *Ceramics International*, 45(14), 17653-17661. <https://doi.org/10.1016/j.ceramint.2019.05.331>
- Li, J., Cushing, S. K., Bright, J., Meng, F., Senty, T. R., Zheng, P., . . . Wu, N. (2013). Ag@ Cu₂O core-shell nanoparticles as visible-light plasmonic photocatalysts. *Acs Catalysis*, 3(1), 47-51. <https://doi.org/10.1021/cs300672f>
- Li, J. Y., Han, W. J., & Yang, Z. P. (2021). Synthesis of potato-based carbon quantum dots, mn doping and their application in ag⁺ detection. *Journal Of Synthetic Crystals*, 50(11), 2093-2102.
- Lim, H., Liu, Y., Kim, H. Y., & Son, D. I. (2018). Facile synthesis and characterization of carbon quantum dots and photovoltaic applications. *Thin Solid Films*, 660, 672-677. <https://doi.org/10.1016/j.tsf.2018.04.019>
- Lin, X. Y., Deng, R. J., & Li, H. T. (2022). N-doped carbon dot-based homogeneous fluorescence assay for the rapid detection of copper contamination in food. *Modern Food Science and Technology*, 38(3), 307-313.
- Malik, L. A., Bashir, A., Qureashi, A., & Pandith, A. H. (2019). Detection and removal of heavy metal ions: A review. *Environmental Chemistry Letters*, 17, 1495-1521.

- Mao, H. H., Xue, M. Y., & Han, G. C. (2021). Synthesis, properties and applications of fluorescent carbon dots. *Functional Material*, 52(1), 1053-1063.
- Mindivan, F., & Göktaş, M. (2023). The green synthesis of carbon quantum dots (CQDs) and characterization of polycaprolactone (PCL/CQDs) films. *Colloids and Surfaces A: Physicochemical and Engineering Aspects*, 677, 132446. <https://doi.org/10.2139/ssrn.4489088>
- Omer, K. M., Tofiq, D. I., & Ghafoor, D. D. (2019). Highly photoluminescent label free probe for Chromium (II) ions using carbon quantum dots co-doped with nitrogen and phosphorous. *Journal of Luminescence*, 206, 540-546. <https://doi.org/10.1016/j.jlumin.2018.10.100>
- Pooja, D., Singh, L., Thakur, A., & Kumar, P. (2019). Green synthesis of glowing carbon dots from Carica papaya waste pulp and their application as a label-free chemo probe for chromium detection in water. *Sensors and Actuators B: Chemical*, 283, 363-372. <https://doi.org/10.1016/j.snb.2018.12.027>
- Rong, M.-C., Zhang, K.-X., Wang, Y.-R., & Chen, X. (2017). The synthesis of B, N-carbon dots by a combustion method and the application of fluorescence detection for Cu²⁺. *Chinese Chemical Letters*, 28(5), 1119-1124.
- Tian, W. K., Qin, X. L., & Xie, Y. (2023). Preparation and properties of oxidized konjac glucon-chitosan composite films. *Food and Fermentation Industry*, 49(22), 1-10.
- Xiang-Yi, D., Ya-Li, F., Dong-Sheng, H., Zhang, Z.-Y., De-Feng, L., & Ru-An, C. (2020). Synthesis of functionalized carbon quantum dots as fluorescent probes for detection of Cu²⁺. *Chinese Journal of Analytical Chemistry*, 48(10), e20126-e20133. [https://doi.org/10.1016/s1872-2040\(20\)60054-8](https://doi.org/10.1016/s1872-2040(20)60054-8)
- Ye, Q., Yan, F., Luo, Y., Wang, Y., Zhou, X., & Chen, L. (2017). Formation of N, S-codoped fluorescent carbon dots from biomass and their application for the selective detection of mercury and iron ion. *Spectrochimica Acta Part A: Molecular and Biomolecular Spectroscopy*, 173, 854-862. <https://doi.org/10.1016/j.saa.2016.10.039>

Online Science Publishing is not responsible or answerable for any loss, damage or liability, etc. caused in relation to/arising out of the use of the content. Any queries should be directed to the corresponding author of the article.